Available online at www.sciencedirect.com
ScienceDirect
Journal of Computational Physics 227 (2008) 6598–6611
JOURNAL OF COMPUTATIONAL PHYSICS
www.elsevier.com/locate/jcp

Scaling the fractional advective–dispersive equation for numerical evaluation of microbial dynamics in confined geometries with sticky boundaries

R. Parashar [a], J.H. Cushman [b,c,*]

[a] Department of Civil Engineering, Purdue University, West Lafayette, IN 47907, USA
[b] Department of Earth and Atmospheric Sciences, Purdue University, West Lafayette, IN 47907, USA
[c] Department of Mathematics, Purdue University, West Lafayette, IN 47907, USA

Received 11 July 2007; received in revised form 16 January 2008; accepted 17 March 2008
Available online 25 March 2008

Abstract

Microbial motility is often characterized by 'run and tumble' behavior which consists of bacteria making sequences of runs followed by tumbles (random changes in direction). As a superset of Brownian motion, Levy motion seems to describe such a motility pattern. The Eulerian (Fokker–Planck) equation describing these motions is similar to the classical advection–diffusion equation except that the order of highest derivative is fractional, $\alpha \in (0, 2]$. The Lagrangian equation, driven by a Levy measure with drift, is stochastic and employed to numerically explore the dynamics of microbes in a flow cell with sticky boundaries. The Eulerian equation is used to non-dimensionalize parameters. The amount of sorbed time on the boundaries is modeled as a random variable that can vary over a wide range of values. Salient features of first passage time are studied with respect to scaled parameters.

Keywords: Levy motion; Microbial dynamics; Sticky boundaries; Stochastic ordinary differential equations; Fokker–Planck non-dimensionalization

1. Introduction

From the perspective of human health, it is imperative that we develop a predictive capability for microbial evolution in pores and porous media. More generally, advection, diffusion, adsorption and other transport modes must be put into a mathematical framework to evaluate the fate of individual microbes and microbial communities as they travel through a porous body. Much of the past effort to model microbial dynamics in porous media is based upon the classical advection–diffusion equation (ADE) subject to rate limited adsorption [1–3]. Unfortunately, even for passive scalars, the ADE is not applicable to most natural porous media [4].

* Corresponding author. Address: Department of Earth and Atmospheric Sciences, Purdue University, West Lafayette, IN 47907, USA. Tel.: +1 7657433958.
E-mail address: jcushman@purdue.edu (J.H. Cushman).

0021-9991/$ - see front matter © 2008 Elsevier Inc. All rights reserved.
doi:10.1016/j.jcp.2008.03.021

Microbes being living organisms, are motile entities [5–7]. Studies suggest that the effect of motility on the dispersive process is significant and is intimately tied to the flow factors [8,9]. Within a single pore, microbial transport seems to agree with prediction from the ADE only if some kind of fitting parameter is introduced [2,10]. A review of various established methods to model microbial transport may be found in [11].

We focus here on the mathematical treatment of the Lagrangian dynamics of a single microbe or a system of such particles in low concentration. Simulations are performed within a single slit-pore to model the movement of a motile particle as it is transported by an advecting bulk fluid. When the particle touches a wall it sticks for a period of time before being released back into the fluid. An α-stable distribution is used to model the sticking time because of its heavy tail. Levy motions are employed to model the motile particles within the pore. These distributions are renormalizable and hence may be upscaled to complex porous bodies [12,13].

In subsequent sections we discuss the typical pattern of microbial motility and adhesion, introduce α-stable Levy motion with their corresponding stochastic differential equations (SDE) and their fractional Fokker–Planck equations. Realizations of the SDE are generated between two infinite parallel surfaces subject to wall stickyness. Results of the numerical study are presented and discussed in the context of a nondimensional parameterization associated with the underlying Fokker–Planck equation.

2. Microbial dynamics

Microbial transport in porous media involves a number of complex and interacting processes [11]. Because microbes are living organisms, their transport in porous media is far more complex than an abiotic colloid. Microbial transport in porous media is affected by not only advection and hydrodynamic dispersion, but also by a number of strictly biological processes. For many of these processes, no definitive correlation with the overall transport process has been established [11]. However, the net resultant of these processes imparts a self-propagating motile character to a microbe [6]. Microbial motility and other physiochemical and biological processes also give rise to adhesion with pore walls. Adhesion is the first step in biofilm formation and as such is a very important process for systems where biofilm development or impediment is desired [14].

Microbes are often equipped with swimming devices. A typical example is a filament attached to a rotary motor [6], the combination of which is called a flagella. The movement of the flagella imparts a run and tumble behavior to the microbe [6,9]. This behavior consists of sequence of runs when all motors rotate together and flagella coalesce to form a bundle. When one or more of the rotary motors changes direction, it results in flagellar dispersion and consequently the microbe tumbles. The change in direction by a tumble is approximated as uniformly random. The microbes thus execute a self-propelled random walk, and it has been shown that the length of the steps may depend on energy gradients [6].

The run and tumble nature of microbial motility has an enhancing effect on the diffusion of colonies and passive scalars residing in surrounding medium. It has been observed that the diffusion process is superdiffusive with mean-square displacement growing faster than linear in time [9]. The extent of departure from Fickian diffusion has been shown to be a function of microbial concentration [9,15], viscosity of the medium [5,16], and pore geometry [17]. As mentioned above, it is also weakly tied to spatial gradients of chemical attractants or repellants [6]. Hence for dilute concentrations of microbes swimming through a given fluid at standard conditions in an experimental flow cell, a probability distribution can be applied to describe the motility pattern. It has been observed that Levy motion defined by α-stable probability distributions of increments best describes the runs and tumbles of microbial motion [6,18,19]. The mixing measure within the definition of a Levy process may be employed to account for microbe food (energy) sources by skewing the movement along a gradient. In essence, Levy motion is a superset of Brownian motion, but unlike Brownian motion, particles undergoing Levy motion take jumps of varying lengths after each time interval Δt. The probability of occurrence of extreme events (very long jumps) is tied to the stability parameter α.

3. Microbial adhesion

It has been observed that the tendency of microbes to attach to surfaces profoundly influences their transport characteristics [8,20]. The process of adhesion of microbes to solid surfaces has been seen to be guided by flagellar movement and flow velocity, amongst other relevant chemical and biological considerations [14]. A

summary of various physiochemical and biological processes that govern the adhesion and other transport characteristics of microbes are presented in [11].

Analysis of the breakthrough curves (travel time to, or concentration at a control plane) have suggested that the sorption process is dominated by both reversible and irreversible adhesion [20]. Experimental observations and simulations have also confirmed that the detachment process results in an elution curve with a long and thin tail [3,8], implying that a fraction of microbes nearly irreversibly attach. An overview of current approaches used to model microbial attachment and detachment is presented in [21]. It has been proposed that linking attachment and detachment rates to metabolic activity and growth of the substrate is vital to improvements in quantitative analysis of microbial adhesion. In absence of such cause-effect relations, the current models which are empirical in nature, fall short of an accurate characterization of the slow elution curves of microbial detachment. Bonilla and Cushman [18] have recently proposed using power law scaling for waiting times for microbes. This approach enables one to explain the long-tailed behavior of microbial detachment and is also consistent with the physical and chemical heterogeneities that are invariably present in the system. Successful simulations involving power law trapping times have been used to explain observed trends in transport through porous samples [22–24].

4. α-Stable levy processes and fades

Levy motion is a generalization of the concept of Brownian motion to processes with infinite variance. Classical Brownian diffusion is characterized by a Gaussian distribution. In Levy motion, long flights are interspersed with shorter jumps, resulting in infinite variance and fractal paths. A two dimensional example of 1000 steps in Levy and Brownian motions is shown in Fig. 1. Starting from origin, and owing to some large intermittent jumps, the Levy motion covers a much larger distance than the Brownian.

The transition density for increments in a Levy motion is given by an α-stable distribution [25,26] which is a family of probability distributions characterized by four parameters: α, β, μ, and σ. The μ and σ are shift and scale parameters which do not determine the shape of the distribution. A number of iid random variables have a stable distribution if a linear combination of these variables has the same distribution, except for possibly different shift and scale parameters. Gaussian distributions and symmetric α-stable distributions look very much alike except that the latter is characterized by a heavier tail. Probability density functions and cumulative distribution functions for a few symmetric and centered α-stable distributions are shown in Figs. 2 and 3 respectively. Whereas Gaussian distributions decay quickly, α-stable distributions decrease as $1/x^{1+\alpha}$, where α lies between 0 and 2. The Gaussian distribution corresponds to the case where $\alpha = 2$.

Levy proved a generalization of DeMoive's central limit theorem by removing the assumption of finite variance on iid random variables X_i [27,28]:

$$\lim_{n\to\infty} \frac{X_1 + X_2 + \cdots + X_n - n\mu}{\sigma n^{\frac{1}{\alpha}}} = Y \sim S_\alpha \quad (\sigma = 1, \beta, \mu = 0), \tag{1}$$

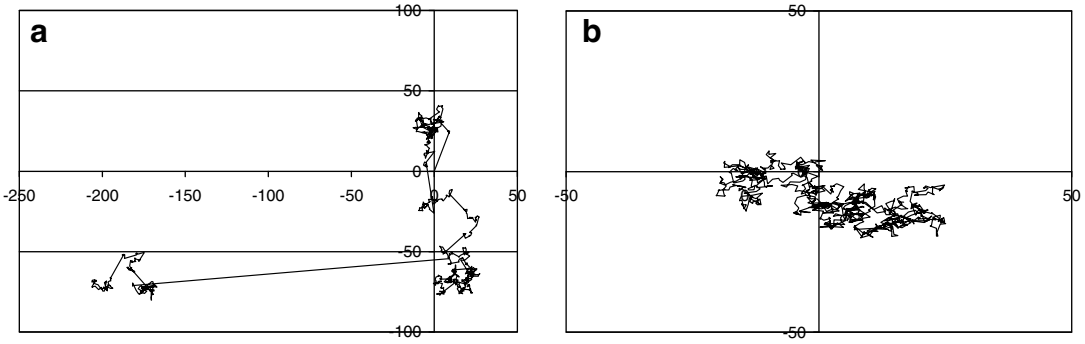

Fig. 1. Trace of (a) Levy motion with $\alpha = 1.5$ and (b) Brownian motion for first 1000 steps starting at (0,0) and having a scale factor of unity.

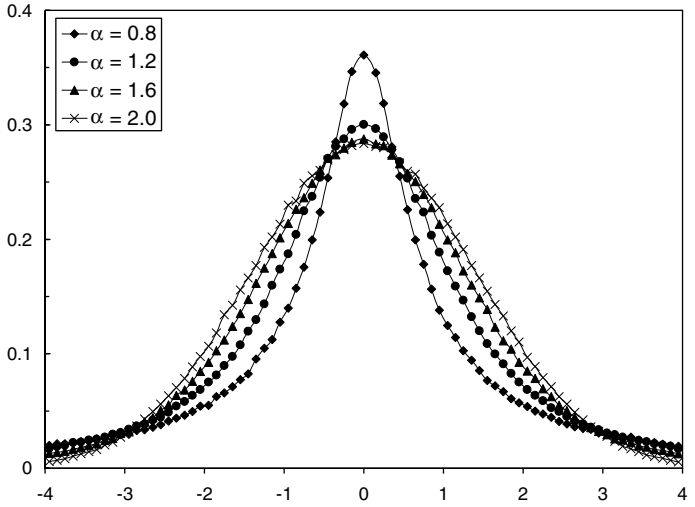

Fig. 2. Probability density function for symmetric and centered α-stable distributions with unit scale factor.

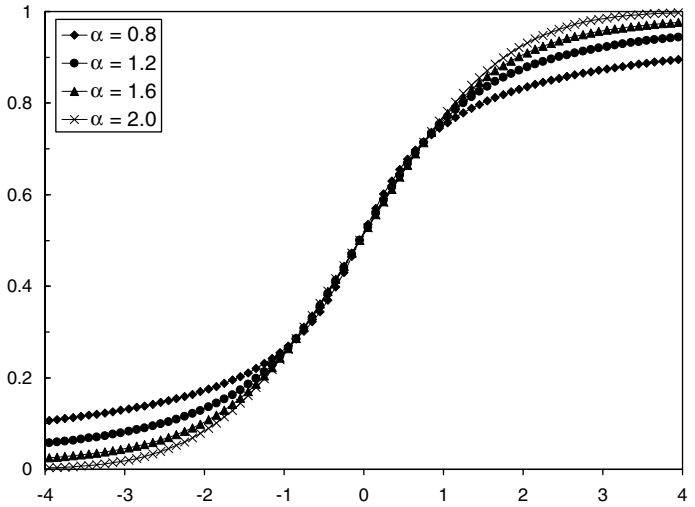

Fig. 3. Cumulative distribution function for symmetric and centered α-stable distributions with unit scale factor.

which states that the centered and normalized sum of iid random variables converges in distribution to an "α-stable" variable with index of stability $0 < \alpha \leqslant 2$, skewness coefficient $-1 \leqslant \beta \leqslant 1$, shift parameter $\mu = 0$, and spread parameter $\sigma = 1$.

By envisioning the sum in Eq. (1) as a random walk with the number of steps, n, equal to the total time divided by the time per move, Δt, we can recast the generalized central limit theorem in the form

$$\lim_{\frac{t}{\Delta t}\to\infty} \frac{X_1 + X_2 + \cdots + X_{\frac{t}{\Delta t}} - vt}{(Bt)^{\frac{1}{\alpha}}} = Y \sim S_\alpha \quad (\sigma = 1, \beta, \mu = 0), \tag{2}$$

where $v = \mu/\Delta t$ and $B = \sigma^\alpha/\Delta t$. The parameters μ and σ appearing in the definition of v and B are the shift and spread parameter for each iid random variable X_i. A stochastic process $\{X(t) : t \geqslant 0\}$ is called an α-stable Levy motion if it has independent increments and $X(t) - X(s) \sim S_\alpha((t-s)^{1/\alpha}, \beta, 0)$ for any $0 \leqslant s < t < \infty$. Since most stable densities cannot be written in real space, they are typically expressed in terms of their Fourier transforms (characteristic functions) as [26]

$$P(k,t) = \exp\left[-\mathrm{i}kX_0 - \left\{Bt|k|^{\alpha}\left(1 - \mathrm{i}\beta\,\mathrm{sign}(k)\tan\frac{\pi\alpha}{2}\right) + \mathrm{i}kvt\right\}\right], \tag{3}$$

where $X_0 = X(0)$ is the initial position of the walk and sign(k) is 1 if $k > 0$, and -1 if $k < 0$. The positive number $(Bt)^{1/\alpha}$ in Eq. (2) indicates that the stable density is invariant upon scaling by $t^{1/\alpha}$. Using a well known property of the characteristic function, namely $\langle X^n(t)\rangle = i^n[\mathrm{d}^n P(k,t)/\mathrm{d}k^n]_{k=0}$, one can easily show that for all $m > \alpha$, $\langle X^m\rangle = \infty$. Hence for any $\alpha < 2$, α-stable densities have infinite variance. However, a finite sampling of the density will yield a finite sample variance. Since the densities are scale invariant with $t^{1/\alpha}$, the sample variance will grow proportional to $t^{2/\alpha}$, i.e. always equal to or faster than Fickian growth. For cases where the distribution is not skewed ($\beta = 0$), Eq. (3) reduces to

$$P(k,t) = \exp[-\mathrm{i}kX_0 - \{Bt|k|^{\alpha} + \mathrm{i}kvt\}]. \tag{4}$$

The value of α in Eq. (3) or (4) determines how non-Gaussian a particular density becomes. As the value of α decreases from a maximum of 2, the tail of the probability density becomes more pronounced (see Figs. 2 and 3). These interesting properties of the α-stable variables have found widespread use in a variety of fields, such as in the study of microbial dynamics [18,19], transport in porous media [29–31], anomalous dispersion [32], and super diffusion in turbulence [33–35].

The Fokker–Planck equation for α-stable Levy motion is fractional [36] and is given by

$$\frac{\partial P(x,t)}{\partial t} = D\nabla^{\alpha}P(x,t), \tag{5}$$

where $D = B/|\cos(\pi\alpha/2)|$ and $P(x, t = 0) = \delta(x - x_0)$. In real space the fractional Laplacians are integrodifferential operators, and hence Eq. (5) describes a spatially nonlocal process. When infinite bounds are used, the fractional Laplacian of order α ($\alpha \in (0, 2]$, $\alpha \neq 1$) for $f(x, t)$ is expressed in 3-dimension as [13,32]

$$(\nabla^{\alpha}f)^{\wedge} = \left[\int_{\|s=1\|} (\mathrm{i}\langle k,s\rangle)^{\alpha} M(\mathrm{d}s)\right]\hat{f}(k,t), \tag{6}$$

where $(\cdot)^{\wedge}$ represents Fourier transform

$$\hat{f}(k,t) = \int_{R^3} \mathrm{e}^{-\mathrm{i}\langle k,x\rangle} f(x)\,\mathrm{d}x \tag{7}$$

and $M(\mathrm{d}s)$ is an arbitrary probability mixing measure on the unit sphere $\{s \in R^3 : \|s\| = 1\}$.

A spatial fractional derivative describes particles that move with long-range spatial dependence or high velocity variability [25]. If a one-dimensional random walk is considered as a motion on an infinite lattice, then a larger-order fractional derivative places more weight on nearer cells and probability of jumps to distant cells decrease very quickly with distance. Conversely, lower-order fractional derivatives place relatively less weight on nearer cells and probability of jumps to distant cells decrease slowly with distance. Like ordinary derivatives, the fractional integrodifferential operators are linear operators but differ in some other important properties such as the fractional derivative of a constant is not zero.

5. Numerics

We take a Lagrangian perspective throughout the remainder of this manuscript; that is, we solve the stochastic Levy driven ODE with parabolic drift. We do so because we are unable to formulate the Eulerian statement of the sticky-wall boundary conditions.

As already mentioned, it is well known that many species of microbes divide their time between a motile free swimming phase and a sorbed phase in which they may exist in a biofilm or attach to a surface. The motion of a free-swimming microbe relative to the moving fluid consists of straight runs followed by tumbles (random changes in direction) [6], resembling to the typical trace of a Levy flight [37]. The example shown in Fig. 4 compares the path of an *E. Coli* cell and that of a tracer executing a 1.2-stable Levy motion.

We model a microflow chamber as an infinite slit-pore. Hence equations of flow between two parallel plates apply to our conceptual domain. Particle transport is modeled as a Levy motion with sticky boundaries. The

Fig. 4. Comparison between a swimming *E. Coli* and a Levy motion with $\alpha = 1.2$ (adapted from Berg, Phys. Today, January 2000 [6]).

parameters for the Levy motion can be obtained from the finite-size Lyapunov exponent [38,39]. The local sorption time is modeled as the absolute value of an α-stable distribution. Our numerical model releases particles at the origin and follows them to a passage plane located some distance downstream. Particles executing multidimensional random motion are liable to cross the passage plane multiple times. The first passage time (FPT) is a quantity of greater interest and under certain circumstances can be tied to the breakthrough curve.

A schematic of the computation cell is shown in Fig. 5. Particles are transported by a Levy process with drift. The jump length is modeled as a symmetric and centered α-stable distribution whereas the adsorbed time is modeled as the absolute of a symmetric and centered α-stable distribution. The top and bottom walls are separated by a distance $2b$ in the y-direction. A passage plane is located at a distance L in the direction of the drift.

At time $t = 0$, particles are released from the source and start swimming and drifting. The angle of swim (flight) after each small time step interval, Δt, is uniformly distributed over a unit sphere at the current location of the particle. The displacement vector for the special case of zero sorption is described by the stochastic equation $X(t) = X(0) + \int_0^t v(X(r))\,\mathrm{d}r + L(t)$, where v is the Poiseuille flow velocity and L is a Levy process which accounts for self-motility. If α_f and σ_f are the parameters of the Levy motion (flight) in the fluid phase and α_w and σ_w are the parameters of the α-stable distribution waiting time (sorbed time) at the walls, then the transport process is computed as follows: (i) generate uniform iid angles; (ii) generate the α-stable flight length, $S_{\alpha f}(\sigma_f, 0, 0)$, using the Chambers, Mallows-Stuck (CMS) algorithm [40] (see Appendix A); (iii) add flight length vector to the current position of the particle; (iv) check if the particle has hit one of the walls, and if so, then modify the length computed in step (ii) and compute the new position vector; (v) compute and the drift from Poiseuille flow based upon the new position of the particle; (vi) if a particle has hit one of the walls in step (iv), then compute its waiting time, $|S_{\alpha w}(\sigma_w, 0, 0)|$, using CMS algorithm and insert it into the clock; (vii) test if the particle has reached the passage plane located downstream; (viii) repeat.

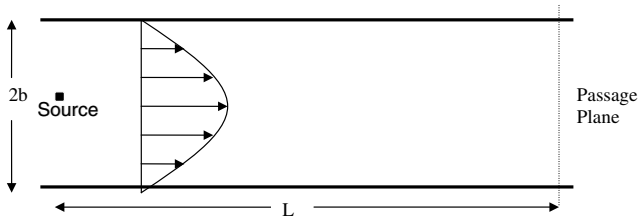

Fig. 5. Schematic of the domain of computation.

To capture the long-tailed behavior of an α-stable distribution, it typically requires on the order of 10^5 particles with each particle on an average experiencing $\sim 10^3$ steps. Besides the distribution parameters (α_f, α_w, σ_f, σ_w), and the length and the time scale, there are two other geometric parameters (b and L) and the fluid properties (pressure gradient and viscosity) that govern the transport process. To examine the behavior of FPT as a function of these variables is a tedious exercise and gives little insight into the mechanism of transport. Hence parameters were grouped together to form suitable non-dimensional numbers and a sensitivity analysis was carried out. This was accomplished by employing the fractional Eulerian equation with sticky boundaries.

6. Non-dimensionalization

As discussed earlier, the Fokker–Planck equation for an α_f-stable Levy process in an infinite domain can be written as a two-dimensional fractional advection–diffusion equation

$$\frac{\partial C}{\partial t} = D\nabla^{\alpha_f} C - v\frac{\partial C}{\partial x}, \tag{8}$$

where C is the concentration of particles at any given location x and t, D is coefficient of diffusion as described in Eq. (5), and v is the drift velocity in the x-direction.

By defining the following non-dimensional parameters

$$X = \frac{x}{L}, \tag{9a}$$

$$T = \frac{vt}{L}, \tag{9b}$$

$$Y = \frac{y}{b}, \tag{9c}$$

$$P = \frac{vL^{\alpha_f - 1}}{D}, \tag{9d}$$

and

$$R = \frac{b^{\alpha_f}}{(DL/v)}, \tag{9e}$$

Eq. (8) can be re-written as

$$\frac{\partial C_0}{\partial T} = \frac{1}{P}\frac{\partial^{\alpha_f} C_0}{\partial X^{\alpha_f}} + \frac{1}{R}\frac{\partial^{\alpha_f} C_0}{\partial Y^{\alpha_f}} - \frac{\partial C_0}{\partial X}, \tag{10}$$

where C_0 is the normalized C with respect to the initial concentration. The non-dimensional parameter P is analogous to the Peclet number encountered in a classical advection–diffusion equation. The parameter R can be interpreted as the ratio between width of the pore and transverse dispersive length. Note that R can be rewritten as $R = (vb^{\alpha_f - 1}/D)(b/L)$ in comparison to Eq. (9d). A smaller value of R will mean that the boundaries of the domain impose a higher restriction on the evolution of plume in the transverse direction. Hence R acts as a constricting agent to the transverse diffusion of Levy motion. In absence of any stickiness on the walls, Eq. (10) suggests $C_0(X, Y; T) = f(\alpha_f, P, R)$.

The correct form of the Eulerian boundary condition at the sticky walls is not obvious, but it is also not necessary information. The frequency of particle attachment to the wall depends on b, α_f and σ_f. The random amount of time for which a particle stays on the wall is a function of α_w and σ_w. Clearly α_w, owing to character of an α-stable distribution, will serve as an independent parameter in the determination of C_0. The other non-dimensional parameter which is introduced by the presence of sticky boundaries can be deduced if a way is found to relate the average amount of time a particle stays on the wall to the average amount of time it spends in the fluid phase. For this, consider the moment at which a particle leaves the wall and re-enters the fluid after getting attached for the very first time. A single step will on average take the particle to a distance of $\mu\sigma_f$ from the wall, where μ is a proportionality coefficient based primarily on α_f. For α_f values higher than 1.2, μ lies between 1.1 and 3 [25]. The number of steps required for the particles to reach one of the walls can be shown

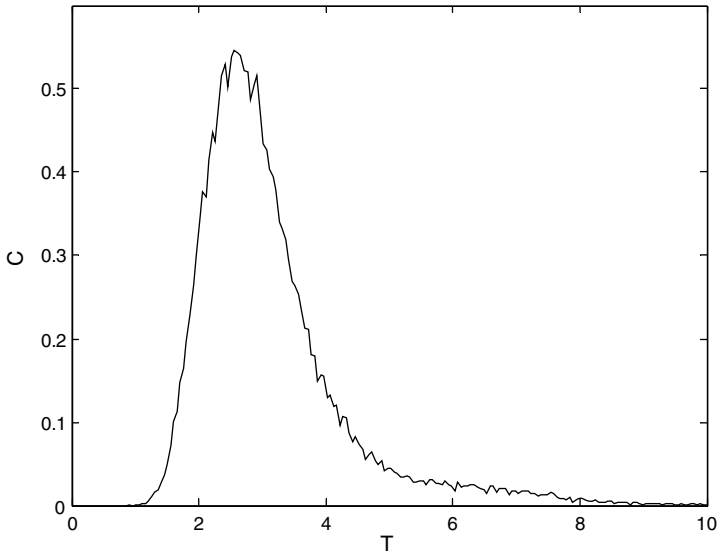

Fig. 6. A typical non-dimensional first passage time density.

to be proportional to $(2b/\sigma)^{\alpha_f/2}$ if μ is much smaller than $2b$ [41]. Using results from [42], the average number of steps can be computed by taking the expected value to yield

$$N_S = \frac{2^{1+\alpha_f/2}\Gamma\left(\frac{1}{2}+\frac{\alpha_f}{4}\right)\Gamma(-1/2)}{\alpha_f\sqrt{\pi}\Gamma(-\alpha_f/4)}\left(\frac{2b}{\sigma}\right)^{\alpha_f/2}. \tag{11}$$

The number of total hits that a particle is expected to have with either of the walls can now be estimated by dividing average of the total number of steps for a particle between the source and the passage plane by the quantity N_S computed in Eq. (11). If Δt is the time step between successive jumps, then the expected number of total hits is given by

$$N_H = \frac{L}{v\Delta t N_S}. \tag{12}$$

A non-dimensional quantity S can now be formulated which is a measure of ratio between average amount of time spent on the wall versus average amount of time spent in the fluid phase. For this purpose, N_H is multiplied by the expected waiting time and then divided by the expected time of travel for a particle in fluid phase to the passage plane given it started at the source:

$$S = \frac{N_H\left[\frac{2\Gamma(1-1/\alpha_w)}{\pi}\sigma_w\right]}{(L/v)}. \tag{13}$$

A large value of S will therefore be associated with walls offering higher degree of stickiness. Non-dimensional concentration in the presence of sticky boundaries can be written as $C_0(X, Y; T) = f(\alpha_f, \alpha_w, P, R, S)$. The first passage time (FPT) density is found at $X = 1$ by integrating the result from $Y = -1$ to $Y = 1$. A typical non-dimensional FPT density exhibiting a long-tailed behavior is shown in Fig. 6. To verify the correctness of non-dimensional formulation, numerous numerical simulations were performed by changing system variables while leaving non-dimensional parameters unchanged. It was observed that the FPT densities matched exactly to each other as long as the set of five non-dimensional parameters remained fixed.

7. Results and discussion

The non-dimensional FPT density is a function of five non-dimensional parameters, namely, α_f, α_w, P, R, and S. A sensitivity analysis of FPT density with respect to these five parameters provides insight into the

comparative importance of different mechanisms of transport and will help in differentiating regimes of flow where a certain variable will play a more significant role in influencing the FPT density than others. Since the FPT densities depend on a Levy motion, they invariably have a slowly decaying tail. Moments higher than the first are infinite for processes governed by an α-stable distribution with $\alpha > 1$. However, one can still talk about skewness in relative sense by comparing mean first passage time (MFPT) with the time to peak, T_P. Similarly, finite central portions of the FPT density can be analyzed to qualitatively examine the spread. In Fig. 7, for fixed α_f and α_w, we have presented plots of MFPT, T_P, and width of central 80% of FPT density (T_W) as a function of P for different values of R and S. A set of similar figures (not shown here for brevity) were constructed for other values of α_f and α_w.

MFPT describes the retardation that the centroid of the breakthrough curve experiences. Comparative values of MFPT and T_P can be used to study the skewness while T_W is a representative measure of the spread. These three statistical quantities are discussed in the following paragraphs with reference to the trends observed in the set of figures constructed in manner similar to Fig. 7.

(i) *MFPT*: Adsorption (S) affects the MFPT by delaying the arrival of particles. However, the sensitivity of the MFPT with respect to S decreases very rapidly as R increases. A smaller R favors higher MFPT by allowing a larger S to influence the breakthrough curve more strongly. Hence the MFPT increases as S increases and R decreases. However, if S is negligible, R seems to have only a mild effect, and P does not affect the MFPT at all. The mild influence of R on the MFPT in absence of any adsorption can be attributed to the congregation of particles near the boundaries of the pore (Fig. 8).
The insensitivity of the MFPT to P for the zero adsorption case is in accordance with the results found for the classical reactive advection–diffusion equation [43]. However, an increasing P was found to significantly influence an increase in the MFPT for cases where S was 0.03 or 0.1 (medium and high values). For P more than 10, the relation between the MFPT and P appears to be linear irrespective of the order of magnitude of R and S. The interplay of P, R, and S in determining the extent by which MFPT gets delayed suggests that these three non-dimensional parameters influence the breakthrough curve in a

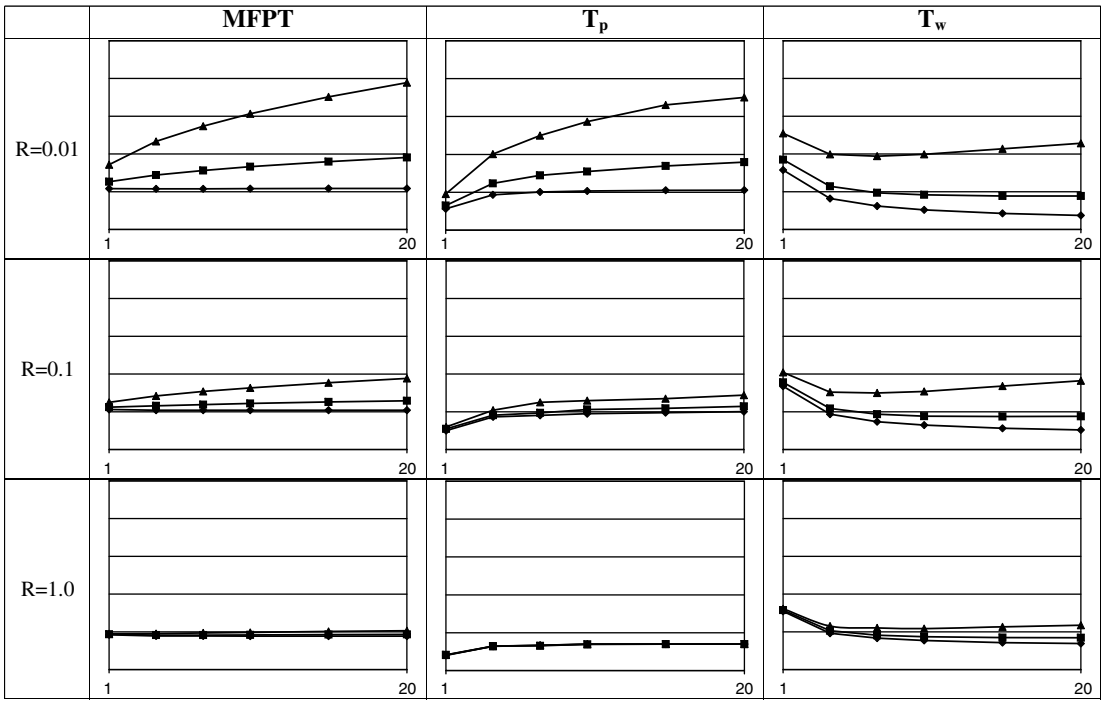

Fig. 7. MFPT, T_P, and T_W as a function of P (varying from 1 to 20) for different values of R. The three lines in each plot correspond to S values of 0.1 (triangle), 0.03 (square), and 0.001 (diamond). The values of α_f and α_w are 1.8 and 1.5 respectively.

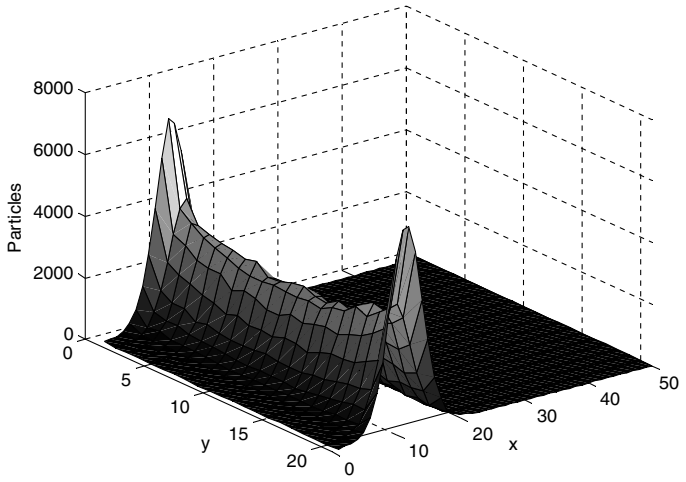

Fig. 8. Particles congregating near walls for a simulation with small R and S equal to zero. Axes have not been non-dimensionalized.

highly coupled fashion. When R is very large ($R = 1.0$ in Fig. 7), a higher or lower S makes little difference in the MFPT as the plume does not spread enough for the boundaries to play a major role. Under these conditions P has no bearing on the value of the MFPT. Similar conclusions can be drawn by letting R become very large in Eq. (10) and then differentiating the characteristic function of the resultant equation to find the first moment.

Sensitivity of the MFPT with respect to α_f can be studied by comparing figures having a fixed α_w while changing α_f. An increase in α_f appears to favor a slight decrease in the MFPT. It is interesting to note that as α_f increases, the expected absolute length of jump decreases, and hence contrary to our observation, a forward biased jump would have exhibited a smaller MFPT for smaller α_f. However, after each jump, our model chooses a jump direction which is uniformly distributed over a unit sphere and therefore for the purpose of computation of the MFPT, the effect of longer jumps in forward direction is annulled by an equal number of longer jumps in the backward direction. The slight increase that we see in the MFPT as α_f decreases is basically a ramification of longer jumps in transverse direction which increases the influence of smaller R and larger S. For larger values of R, where breakthrough curves are slightly influenced by S, a decrease in α_f slightly lowers the MFPT. For the near classical case (α_f close to 2.0) with far-off boundaries ($R = 1.0$) and negligible sorption ($S = 0.001$), the MFPT goes to 1.0 as would be expected from the results of classical advection–diffusion equation [43].

The effect of α_w on the MFPT can be studied by changing that quantity while keeping α_f fixed. One may be tempted to predict that higher α_w will have a decreasing influence on the MFPT because of the smaller averages associated with higher α. However, in the non-dimensional framework, the average time spent on the wall is accounted for by S and hence the effect of changingα_w may not necessary be in accord with dimensional analysis. In fact, an increase in α_w was seen to increase the MFPT as well. This happens because particles with a waiting time distribution characterized by a higher value of α_w spend a shorter amount of time on the wall and are relatively quickly released back into the fluid phase. The faster the release, the higher is the probability of particles accumulating near the wall and negatively influencing the MFPT. However, overall it can be said that the influence of α_f and α_w on the MFPT is fairly small when compared to the influence of P, R, and S. Hence α_f and α_w are not the key factors when examining the sensitivity of the MFPT, although they do a play a major role in determining the value of the MFPT by the virtue of being a part of the definition of P, R, and S.

(ii) *MFPT, T_P, and skewness*: Second- and higher-order moments are mathematically non-existent for transport processes governed by an α-stable Levy motion. However, one can use the information gathered in a finite amount of time to qualitatively speak about the nature of the breakthrough curve. One such important feature is the degree of skewness (asymmetric nature of a breakthrough curve). Skewness can be assessed by comparing the MFPT with the time to peak, T_P. If T_P is smaller than the MFPT,

then the breakthrough curve will have a positive skewness. The rising limb in this case will be shorter (and steeper) than the falling limb and vice-versa when T_P is larger than the MFPT. In all simulation runs, T_P was observed to be smaller than the MFPT. This result held true for all possible combinations of P, R, S, α_f, and α_w. The difference was only that of degree. The gradual release of particles in the falling limb, as compared to the more rapid release of particles in the rising limb, can largely be attributed to particles left in the vicinity of top and bottom walls, owing to both the adsorption phenomenon and the parabolic velocity profile of the advecting fluid (see Fig. 9).

Relative changes or sensitivity of T_P with respect to the five non-dimensional parameters showed similar qualitative trends, but differed quantitatively to what has been discussed for the case of the MFPT. This means that T_P increases rapidly with increasing S and increasing P for cases when R is small. For medium and large R values (0.1 and 1.0), T_P remained fairly insensitive to changes in S and P. One noteworthy difference between the dependence of the MFPT and T_P on P is that a linear trend occurs at a slightly later stage. This becomes more apparent as α_f increases to 2.0.

T_P varies slightly with α_f and increases with increasing α_w. However, an increase in T_P with respect to α_w is more pronounced than that of the MFPT. These slight variations in the behavior of the MFPT and T_P with respect to the five non-dimensional parameters stretch or shorten the gap between the MFPT and T_P and thereby increase of or decrease the amount of skewness one can observe in the breakthrough curves. It was observed that the breakthrough curves are minimally skewed for small values of S irrespective of the value of R. Hence R does not have a marked effect on the skewness unless it is coupled with a non-negligible S. One can think of R as a constricting parameter which impedes the transverse expansion of an evolving plume. However skewness in the final breakthrough curve is often a result of long tails developing behind the centroid of the evolving plume and the non-dimensional parameter R does not aid this occurrence unless coupled with a suitably large S. An increasing P also helps in lengthening the falling limb as it influences the growth of the MFPT more than the growth of T_P. The difference in these two growth rates are non-linear for smaller values of P, but gradually become linear as P increases. For fixed values of P, R, S and α_f, we observe that as α_w increases, the gap between the MFPT and T_P shrinks. Hence a long tailed waiting time distribution has a tailing effect on the non-dimensional breakthrough curve. Sensitivity of skewness with respect to α_f is the same as the sensitivity of the MFPT.

(iii) *T_W and spread*: Spread in a breakthrough curve is important when analyzing the features of a diffusive process. Although the second moment for Levy processes is infinite, one can still gain a fair amount of understanding of the transport mechanism by studying a large central portion of a breakthrough curve.

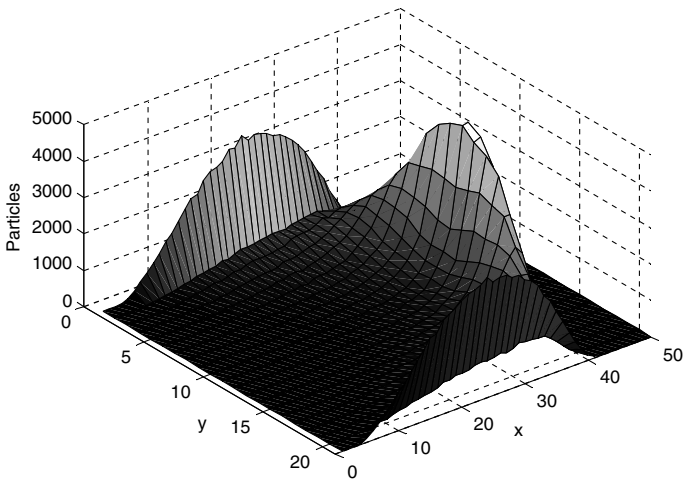

Fig. 9. Trail of particles left at the walls due to adsorption and parabolic velocity profile. Axes have not been non-dimensionalized.

We have chosen to examine the spread of the central 80%. The difference in the location of points on falling and rising limb between which the mid 80% of the particles exit the passage plane is denoted by T_W and plotted in the third column of Fig. 7.

With no or little sorption, it is reasonable to expect that T_W will decrease as P increases. Not surprisingly, this is what is exhibited in all the plots corresponding to $S = 0.001$. An increase in R from 0.01 to 1.0 for negligible sorption ($S = 0.001$) appears to have a non-linear influence on T_W. Depending upon value of α_f, for $S = 0.001$, T_W first increases as R increases from 0.01 to 0.1 and then either decreases (with lower α_f) or remains relatively unchanged (with higher α_f) as R increases from 0.1 to 1.0. This behavior can again be understood if we think of R as a constricting parameter. A smaller R, which means that the boundaries are fairly close when compared to the transverse diffusive length of the evolving plume, impedes long flights. Hence an increase in R, for negligible sorption, has a positive effect on T_W. This effect is more pronounced in cases with smaller α_f. However, as R increases, a majority of particles having started their journey from the center plane of the pore, sample a fairly high velocity field which aids in reducing the spread, T_W. As R increases, one reaches a point where the increase in T_W because of possible long flights is more than accounted for by the decrease in T_W owing to the parabolic velocity field that the particles may sample. It should be emphasized that these results are associated with small S. As S increases from 0.001 to 0.1, a few interesting trends appear in the plots of T_W. Chief among these is an increasing trend in T_W despite an increasing P. Aided by a combination of a higher value of S, or a smaller value of R, or a smaller value of α_f, a rising trend in T_W starts from a point somewhere between $P = 1$ to $P = 10$ depending upon the comparative values of S, R, and α_f. The influence of α_w on this reversal of trend is minimal.

With negligible sorption, smaller values of α_f are expected to have a positive influence on the overall spread, and hence it is not a surprise when that trend continues for cases when sorption is substantial. What is more interesting is that unlike the case with negligible sorption, T_W increases monotonically as R decreases. Though a smaller value of R curtails many of the long flights and has a reducing effect on T_W, in the presence of sorptive boundaries the higher frequency of particles hitting and attaching to the wall leads to a far larger spread. As P increases for cases with constant S, the net amount of adsorbed time increases as well, since S by definition represents a ratio of adsorbed time to the time spent in the fluid phase. The influence of S is strong enough to not only counter, but over compensate for any reduction in T_W that may be brought about by an increase in P.

8. Conclusions

Motile particle transport in a slit-pore was studied numerically using Levy motion and an α-stable distribution to characterize the motility and stickiness of the boundaries, respectively. The advective–dispersive transport process coupled with adsorption at the boundaries leads to a long-tailed first passage time (FPT) density intricately tied to a number of system variables. With the help of the Eulerian Fokker–Planck equation for a Levy motion and the sticky boundary condition, five non-dimensional parameters were derived that control the concentration evolution. Simulations were carried out in Lagrangian framework to compute the non-dimensional FPT densities and its statistical properties representing mean, spread, and skewness. By varying only one of the five non-dimensional parameters, their influence on the FPT density was studied. It was observed that under typical conditions, the non-dimensional parameters affect the mean, spread, and skewness of FPT density in a highly coupled fashion. Hence sensitivity of FPT density with respect to any single non-dimensional parameter is also determined by the relative values of other parameters. A detailed analysis of mean first passage time (MFPT), spread, and skewness was presented. It is hoped that the non-dimensionalization and sensitivity analysis will aid experimentalists in designing experiments and processing the data.

Acknowledgment

This work was financially supported by National Science Foundation under Contracts EAR-0310029 and EAR-0620460.

Appendix A. α-Stable deviate generator

If $Y \sim S_\alpha(\sigma, \beta, \mu)$ and $\alpha \neq 1$, then $Y = \sigma X + \mu$, where $X \sim S_\alpha(1, \beta, 0)$ is a standard stable random variable. To generate a standard stable deviate, the following steps are followed:

(i) Generate a random variable V uniformly distributed on $(-\pi/2, \pi/2)$ and an independent exponential random variable W with mean 1.
(ii) Compute

$$X = S_{\alpha,\beta} \frac{\sin[\alpha(V + B_{\alpha,\beta})]}{[\cos(V)]^{1/\alpha}} \left(\frac{\cos[V - \alpha(V + B_{\alpha,\beta})]}{W} \right)^{(1-\alpha)/\alpha}, \tag{A.1}$$

where

$$S_{\alpha,\beta} = \left[1 + \beta^2 \tan^2 \frac{\pi\alpha}{2} \right]^{1/(2\alpha)} \tag{A.2}$$

and

$$B_{\alpha,\beta} = \frac{\arctan\left[\beta \tan\left(\frac{\pi\alpha}{2}\right)\right]}{\alpha}. \tag{A.3}$$

Equations corresponding to the case of $\alpha = 1$ are not shown here for brevity.

References

[1] R. Lindqvist, G. Bengtsson, Microb. Ecol. 21 (1991) 49.
[2] Y. Tan, J.T. Gannon, P. Baveye, M. Alexander, Water Resour. Res. 30 (12) (1994) 3243.
[3] W.P. Johnson, K.A. Blue, B.E. Logan, R.G. Arnold, Water Resour. Res. 31 (11) (1995) 2649.
[4] J.H. Cushman, Water Resour. Res. 27 (4) (1991) 643.
[5] H.C. Berg, L. Turner, Nature 278 (1979) 349.
[6] H.C. Berg, Phys. Today, January 24 (2000).
[7] S.C. Kuo, J.L. McGrath, Nature 407 (2000) 1026.
[8] A.K. Camper, J.T. Hayes, P.J. Sturman, W.L. Jones, A.B. Cunningham, Appl. Environ. Microbiol. 59 (10) (1993) 3455.
[9] M.J. Kim, K.S. Breuer, Phys. Fluids 16 (9) (2004) L78.
[10] G.M. Hornberger, A.L. Mills, J.S. Herman, Water Resour. Res. 915 (1992).
[11] T.R. Ginn, B.D. Wood, K.E. Nelson, T.D. Scheibe, E.M. Murphy, T.P. Clement, Adv. Water Resour. 25 (2002) 1017.
[12] M. Park, N. Kleinfelter, J.H. Cushman, Phys. Rev. E 72 (2005) 056305.
[13] M. Park, N. Kleinfelter, J.H. Cushman, SIAM Multiscale Model. Simul. 4 (4) (2005) 1233.
[14] J.W. McClaine, R.M. Ford, Biotechnol. Bioeng. 78 (2) (2002) 179.
[15] T.A. Camesano, B.E. Logan, Environ. Sci. Technol. 32 (1998) 1699.
[16] Y. Magariyama, S. Kudo, Biophys. J. 83 (2002) 733.
[17] S.A. Bondi, J.A. Quinn, H. Goldfine, AIChE J. 44 (1998) 1923.
[18] F.A. Bonilla, J.H. Cushman, Phys. Rev. E 66 (2002) 031915.
[19] M. Park, N. Kleinfelter, J.H. Cushman, Geophys. Res. Lett. 33 (2006) L01401.
[20] M.J. Hendry, J.R. Lawrence, P. Maloszewski, Ground Water 35 (4) (1997) 574.
[21] E.M. Murphy, T.R. Ginn, Hydogeol. J. 8 (2000) 14.
[22] G. Drazer, M. Rosen, D.H. Zanette, Phys. A 283 (2000) 181.
[23] G. Drazer, D.H. Zanette, Phys. Rev. E 60 (1999) 5858.
[24] R. Schumer, D.A. Benson, M.M. Meerschaert, B. Baeumer, Water Resour. Res. 39 (10) (2003) 1296.
[25] D.A. Benson, The Fractional Advection–Dispersion Equation: Development and Application, PhD Thesis, University of Nevada, Reno, 1998.
[26] A. Janicki, A. Weron, Simulation and Chaotic Behavior of α-Stable Stochastic Processes, Marcel Dekker, New York, 1994.
[27] P. Levy, Theorie de l'addition des variables aleatories, Gauthier-Villars, Paris, 1937.
[28] W. Feller, An Introduction to Probability Theory and its Application, vol. II, John Wiley, New York, 1971.
[29] S. Painter, Water Resour. Res. 32 (5) (1996) 1323.
[30] D.A. Benson, S.W. Wheatcraft, M.M. Meerschaert, Water Resour. Res. 36 (6) (2000) 1403.
[31] M.G. Herrick, D.A. Benson, M.M. Meerschaert, K.R. McCall, Water Resour. Res. 38 (11) (2002) 1227.
[32] M.M. Meerschaert, D.A. Benson, B. Baumer, Phys. Rev. E 59 (1999) 5026.

[33] M.F. Shlesinger, B.J. West, J. Klafter, Phys. Rev. Lett. 58 (1987) 1100.
[34] J.H. Cushman, M. Park, N. Kleinfelter, M. Moroni, Geophys. Res. Lett. 32 (2005) L19816.
[35] M. Park, J.H. Cushman, J. Comput. Phys. 217 (2006) 159.
[36] D.A. Benson, S.W. Wheatcraft, M.M. Meerschaert, Water Resour. Res. 36 (6) (2000) 1413.
[37] G.M. Viswanathan, S.V. Buldyrev, S. Halvin, M.G.E. daLuz, E.P. Raposo, H.E. Stanley, Nature 401 (1999) 911.
[38] N. Kleinfelter, M. Moroni, J.H. Cushman, Phys. Rev. E 72 (2005) 056306.
[39] R. Parashar, J.H. Cushman, Phys. Rev. E 76 (2007) 017201.
[40] J.M. Chambers, C.L. Mallows, B.W. Stuck, J. Am. Stat. Assoc. 71 (1976) 340.
[41] S.V. Buldyrev, S. Halvin, A.Ya. Kazakov, M.G.E. da Luz, E.P. Raposo, H.E. Stanley, G.M. Viswanathan, Phys. Rev. E 64 (2001) 041108.
[42] C.L. Nikias, M. Shao, Signal Processing with Alpha-Stable Distributions and Applications, John Wiley and Sons, 1995.
[43] R. Parashar, R.S. Govindaraju, M.M. Hantush, J. Environ. Eng. – ASCE 133 (9) (2007) 879.